Published in final edited form as:
Colloids Surf B Biointerfaces. 2014 February 1; 114: . doi:10.1016/j.colsurfb.2013.10.009.

Shrinkage of pegylated and non-pegylated liposomes in serum

Joy Wolfram[a,b,*,1], **Krishna Suri**[b,1], **Yong Yang**[b], **Jianliang Shen**[b,c], **Christian Celia**[b,d], **Massimo Fresta**[e], **Yuliang Zhao**[a,f], **Haifa Shen**[b,g], and **Mauro Ferrari**[b,h,*]

Joy Wolfram: jvwolfram@tmhs.org; Mauro Ferrari: mferrari@tmhs.org

[a]CAS Key Laboratory for Biomedical Effects of Nanomaterials & Nanosafety, National Center for Nanoscience & Technology of China, Beijing 100190, China

[b]Department of Nanomedicine, Houston Methodist Research Institute, Houston, TX 77030, USA

[c]MOE Key Laboratory of Bioinorganic and Synthetic Chemistry, School of Chemistry and Chemical Engineering, Sun Yat-sen University, Guangzhou 510275, China

[d]Department of Pharmacy, University G. d'Annunzio of Chieti, Pescara, 66013 Chieti, Italy

[e]Department of Health Science, University Magna Græcia of Catanzaro, Germaneto 88100, Italy

[f]Institute of High Energy Physics, Chinese Academy of Sciences (CAS), Beijing 100049, China

[g]Department of Cell and Developmental Biology, Weill Cornell Medical College, New York, NY 10065, USA

[h]Department of Medicine, Weill Cornell Medical College, New York, NY 10065, USA

Abstract

An essential requisite for the design of nanodelivery systems is the ability to characterize the size, homogeneity and zeta potential of nanoparticles. Such properties can be tailored in order to create the most efficient drug delivery platforms. An important question is whether these characteristics change upon systemic injection. Here, we have studied the behavior of phosphatidylcholine/cholesterol liposomes exposed to serum proteins. The results reveal a serum-induced reduction in the size and homogeneity of both pegylated and non-pegylated liposomes, implicating the possible role of osmotic forces. In addition, changes to zeta-potential were observed upon exposing liposomes to serum. The liposomes with polyethylene glycol expressed different characteristics than their non-polymeric counterparts, suggesting the potential formation of a denser protein corona around the non-pegylated liposomes.

Keywords

Liposomes; Dynamic light scattering; Size; Serum; Polydispersity index; Zeta potential

1. Introduction

Several nanodelivery systems have already received clinical approval and many more are currently undergoing clinical trials [1]. Liposomes account for a major portion of the nanomedicine products on the market. Currently, 13 liposomal drugs have been approved and many more are enrolled in clinical trials [2,3]. Liposomes are composed of amphipathic

*Corresponding authors. Tel.: +1 713 441 1839/+1 713 441 8439; fax: +1713 441 3655.
[1]These authors contributed equally.

phospholipids that form a bilayer structure, which allows for the entrapment of both hydrophilic and hydrophobic agents [4]. By changing the phospholipid composition the characteristics of liposomes can be modified [5]. In addition, polymers, such as polyethylene glycol (PEG) can be self-assembled into the lipid bilayer, thereby forming 'stealth liposomes' [6,7]. PEG creates a steric barrier around the liposomal surface that hinders the binding of plasma proteins, hence shielding the liposome from immunological recognition and loss of stability. The stealth effect results in longer blood circulation times, which can improve therapeutic efficacy [8].

Properties of nanoparticles, such as the size and charge, play a pivotal role in overcoming biological barriers and reaching the target region [9]. Hence, accurate measuring and tailoring of such properties, based on the intended therapeutic modality, could be a key factor for the success of liposomes. Currently, there is an ongoing debate within the scientific community regarding how the properties of nanoparticles change within bodily fluids. Even in the presence of PEG, it is possible for a biomolecule corona to form around nanoparticles [10,11]. This corona impacts and dictates the behavior of nanoparticles in biological milieus [12–17]. An emerging idea is that nanoparticles should be classified based on their interactions with the *in vivo* environment, instead of being characterized according to the bare properties of the particles [13–15].

In this work we focus on elucidating how the properties of different sized pegylated and non-pegylated phosphatidylcholine (PC)/cholesterol liposomes change in the presence of serum. Here, we have simulated physiological conditions by incubating liposomes in fetal bovine serum at body temperature (FBS). Dynamic light scattering has been used to characterize the lipid-based particles, as this is the most convenient method to determine the dimensions of particles in solution [18]. Liposomal size, homogeneity and zeta potential have been measured in response to varying concentrations of serum. The changes in these parameters have also been monitored over time. The various measurements have been analyzed to see whether concentration-dependent or time-dependent trends can be observed.

2. Materials and methods

2.1. Materials

Cholesterol was purchased from Sigma Aldrich, while 1,2-dipalmitoyl-*sn*-glycero-3-phosphoethanolamine (DPPE) and 1,2-distearoyl-phosphatidylethanolamine-methyl-polyethyleneglycol conjugate-2000 (DPPEmPEG2000) were obtained from Avanti polar lipids (#850705P and #880160P). phosphatidylcholine (PC) was obtained from Lipoid (#S100). Silica nanospheres were acquired from Microspheres–Nanospheres (#141112-10).

2.2. Liposome preparation

Two different formulations of liposomes were prepared: (i) PC, cholesterol, DPPEmPEG-2000 (6:3:1 molar ratio) and (ii) PC, cholesterol, DPPE (6:3:1 molar ratio). The compositional elements were dissolved within a round bottom flask using a mixture of chloroform and methanol (2:1; v/v). The lipid films were formed with a Rotovapor (R-215, Buchi Corporation) set at 180 rpm and 200 mbar with a 50 °C water bath. The films were allowed to dry overnight, and were subsequently hydrated with phosphate buffered saline (PBS; 1 ml/20 mg phospholipids). Hydration was performed by heating the formulation three times within a 60 °C water bath (3 min) followed by vortex mixing (3 min). To increase homogeneity and to collect liposomes of different sizes, the formulations were extruded through polycarbonate membranes with the following pore sizes: (i) 400, 200 and 100 nm, (ii) 400, 200, 100 and 80 nm and (iii) 400, 200, 100 and 50 nm, using an extrusion device from Lipex Biomembranes (Northern Lipids Inc., Vancouver, BC, Canada).

2.3. Serum incubation

Changes to liposomal characteristics were evaluated in 100%, 60% and 20% FBS (diluted in PBS) at 37 °C. Silica beads (25 mg/ml) were incubated in 100% FBS. 200 μl of the liposomal formulation or silica beads were added to 1 mL of FBS solution. Time course studies up to 12 days were performed with 60% and 100% FBS at 37 °C with stirring (700 rpm). Sterile conditions were maintained throughout the experiment, in order to avoid bacterial contamination that could affect sample readings.

2.4. Dynamic light scattering

For dynamic light scattering analysis samples were prepared at a 1:50 dilution and measured with a Zetasizer Nano ZS (ZEN 3600, Malvern Instruments). The variables measured were size (Z_{avg}, diluted in Milli-*Q* water or PBS), polydispersity index (PDI, diluted in Milli-*Q* water or PBS), and zeta potential (ζ, diluted in phosphate buffer). For each sample five measurements were taken with 15 runs per measurement. Size is presented in terms of Z_{avg}, which represents the mean hydrodynamic diameter with respect to the range of intensities measured using dynamic light scattering. The Z_{avg} value is derived using Cumulants analysis in which particle size is calculated with the Stokes-Einstein equation:

$$D=\frac{k_B T}{6\pi\eta_0 r_h}$$

where D is the diffusion coefficient, k_B is the Boltzmann constant, T is temperature, η_0 is the viscosity of water at a given temperature and r_h is the hydrodynamic radii. This equation relates the light scattering observed due to Brownian motion with particle size. After obtaining the range of backscattering intensities, the correlation curve is applied to the following exponential fitting expression to obtain the Z_{avg} and PDI values:

$$G_2(\tau)=A[1+B\exp(-2\Gamma\tau)$$

where τ is the delay time, A is the amplitude of the correlation function, B is the baseline and Γ is the decay rate.

Zeta potential (ζ) was determined from the electrophoretic mobility values obtained through laser Doppler velocimetry (LDV). The instrument calculated the zeta potential values through Henry's equation:

$$U_E=\frac{2\varepsilon z f(ka)}{3\eta}$$

where U_E is electrophoretic mobility, z is zeta potential, η is viscosity, ε is the dielectric constant and *f(ka)* is Henry's function. Since zeta potential measurements were performed in a folded capillary cell in aqueous media, the Smoluchowski approximation value of *f(ka)* (1.5) was applied.

3. Results and discussion

3.1. Pegylated and non-pegylated liposomes of different sizes

Extrusion through membranes with 100 nm, 80 nm and 50 nm pores yielded liposomes of three different size categories (Table 1). The non-pegylated liposomes were larger in size than their pegylated counterparts. All formulations displayed low PDI values (<0.06), suggesting a homogenous size distribution. The zeta potential of the non-pegylated liposomes was around -5 mV, while the pegylated liposomes had a slightly lower zeta potential of approximately −10 mV. Upon storage in 4 °C the liposomes remained stable, as was evident from relatively consistent size, PDI and zeta potential values (Fig. 1). Dynamic light scattering revealed that the PDI and size of the liposomes were similar upon dilution with Milli-*Q* water or PBS (Fig. 2).

3.2. Serum-induced changes in liposome size

Upon contact with serum the non-pegylated and pegylated liposomes shrank in size. The pegylated liposomes exhibited a more dramatic decrease in size (16 nm in 100% FBS) in comparison to their non-pegylated counterparts (11 nm in 100% FBS) (Fig. 3). All formulations displayed a single intensity peak, which is required for the accurate interpretation of the Z_{avg}. Interestingly, the decrease in size was independent of liposomal size, as all formulation of the same composition showed an almost identical reduction in the diameter when exposed to serum. However, the decrease in size was dependent on the serum concentration (100%, 60% or 20%), where liposomes exposed to 100% FBS displayed the greatest change in size (Fig. 3c).

There are several ways in which serum proteins may interact with liposomes. One way is through the formation of a corona, which entails the binding of biomolecules to the surface of nanoparticles [12,13,15,16]. This effect is likely to cause an increase in the size of liposomes. Another way that serum may impact liposomes is trough osmotic pressure caused by proteins that are impermeable to the liposomal membrane, hence causing water to escape from the liposomal core and subsequent shrinking of the vesicle. It is possible that the latter effect is responsible for the serum-induced reduction in liposomal size. Previously, it has been shown that liposomes exposed to a solution of ions decrease in size, due to osmotic pressure [19–21], supporting the notion that osmotic pressure acts upon liposomes. The less dramatic decrease in size seen with the non-pegylated liposomes, in comparison to the pegylated ones, could be due to a more extensive protein corona forming around the non-polymeric liposomes, resulting in a thickening of the liposomal surface and a subsequent increase in diameter. Pegylated surfaces, on the contrary, can exhibit repulsive forces against serum proteins [22–24], thus hindering the formation of a dense protein corona.

Due to methodological limitation samples could not be measured directly in FBS, as serum alone shows multiple intensity peaks. Therefore, prior to reading the samples by dynamic light scattering, they were diluted in Milli-*Q* water (1:50). Hence, the actual FBS concentration upon measuring the samples was considerable less (∼2%, ∼1% and 0.4%), suggesting that the real serum-induced change in size could be different and even more dramatic than depicted here. It is also possible that the presence of serum components could influence the light scattering pattern. Therefore, to further address the effect of serum proteins, an additional control experiment was performed using silica nanospheres, which are not prone to size changes due to osmotic stress. The results indicate that silica beads, unlike liposomes, increase in size when exposed to 100% FBS (Fig. 4). This result suggests that the observed shrinkage of liposomes is not a consequence of serum proteins interfering with the light scattering pattern.

3.3. Serum-induced changes in homogeneity and zeta potential

The PDI of non-pegylated and pegylated liposomes increased in serum, implicating a decrease in homogeneity. As the serum concentration was elevated the PDI became larger (Fig. 5). The serum-induced change was independent of liposomal size. The pegylated liposomes displayed a greater change in PDI, in comparison to the non-pegylated liposomes (Fig. 5d). The zeta potential for the non-pegylated liposomes decreased in serum, while it remained relatively consistent for the pegylated liposomes (Fig. 6), possibly implicating the formation of a protein corona around the non-polymeric liposomes.

3.4. Time-course studies in serum

Liposomes were incubated in 100% and 60% serum for 12 days. Within the first few hours the liposomes exhibited a reduction in size and an increase in PDI, where after these values stabilized (Fig. 7). After 12 days the PDI for pegylated and non-pegylated liposomes increased. Similarly, the zeta potential for non-pegylated liposomes dropped dramatically on the 12th day, while it remained relatively stable for the pegylated liposomes. These changes were greater when the liposomes where incubated in 100% FBS (Fig. 7a) in comparison to 60% FBS (Fig. 7b). Both liposomal formulations did not undergo aggregation or break down in serum, as was evident from the consistent Z_{avg} values and the presence of a single intensity peak in the dynamic light scattering measurements. Cholesterol has previously been shown to increase the stability of liposomes [25], which may explain why the non-pegylated liposomes stayed intact in FBS.

The notion that certain liposomes decrease in size in the presence of serum can have implications for the design of therapeutic nanodelivery systems. The major challenge for the successful delivery of drugs *in vivo* is overcoming multiple biological barriers [9]. Many of these biological barriers have size exclusion. Namely, the successful penetration of nanoparticles through vasculature and the avoidance of clearance by organs, such as the liver and kidneys, are highly dependent on size. For instance, it has previously been shown that nanoparticles over 50 nm in size are unable to penetrate the vasculature of pancreatic tumors [26]. In addition, particles in the 100 nm range have a higher likelihood of accumulating in the liver, while the kidneys clear particles smaller than 5.5 nm [26,27]. As size plays a prominent role in the success of nanocarriers it is important to know the precise dimensions of nanoparticles after systemic administration.

Moreover, the shrinkage of liposomes in response to osmotic forces may have consequences for drug release. Drugs loaded into the aquatic core could potentially be released as the water flows out of the vesicle. Invariably, the reduction in liposomal size also causes the lipid bilayer to compress. Hence, hydrophobic drugs embedded within the bilayer may likewise be released in response to compression. Consequently, it is possible that liposomes may display a burst drug release within seconds after being exposed to proteins in bodily fluids. Furthermore, a protein corona may simultaneously form around the liposome surface, increasing the size of the nanoparticles. In these experiments the liposomal reduction in size, presumably caused by osmotic pressure, was greater than the probable increase in size, arising from the formation of a protein corona. Indeed, the non-pegylated liposomes displayed a smaller reduction in size, potentially suggesting the presence of a thicker biomolecular corona. In essence, this study serves to illustrate that liposomes may drastically change in size within seconds after interacting with serum proteins, while simultaneously maintaining stability and uniform confirmation. Hence, one should be aware of liposomal characteristics in the presence of serum proteins when designing delivery vehicles for systematic administration.

4. Conclusion

We have shown that the characteristics of liposomes can change upon exposure to FBS. The pegylated and non-pegylated formulations displayed a serum-induced size-independent and concentration-dependent reduction in size and homogeneity. The zeta potential of the non-pegylated liposomes dropped in the presence of serum, while the zeta potential for the pegylated liposomes remained relatively consistent. Except for the initial increase in size, all formuations were stable in serum up to 12 days, suggesting that both PEG and cholesterol can act as stabilizing agents. The FBS-induced changes are likely to be caused by osmotic pressure and the formation of a protein corona around the liposomes.

Acknowledgments

The research was supported by funds from the Methodist Hospital Research Institute. Partial funds were acquired from: the Ernest Cockrell Jr. Distinguished Endowed Chair (M.F.), the US Department of Defense (W81XWH-09-1-0212) (M.F.), the National Institute of Health (U54CA143837, U54CA151668) (M.F.), Nylands nation Finland (J.W.), Department of Defense grant W81XWH-12-1-0414 (M.F.) and the State of Texas CPRIT grant RP121071 (M.F. and H.S.). We thank Matthew Landry for assistance with the figures.

References

1. Wagner V, Dullaart A, Bock AK, Zweck A. The emerging nanomedicine landscape. Nat Biotechnol. 2006; 24:1211–1217. [PubMed: 17033654]
2. Chang HI, Yeh MK. Clinical development of liposome-based drugs: formulation, characterization, and therapeutic efficacy. Int J Nanomed. 2012; 7:49–60.
3. Koudelka S, Turánek J. Liposomal paclitaxel formulations. J Controlled Release. 2012; 163:322–334.
4. Zhang L, Gu FX, Chan JM, Wang AZ, Langer RS, Farokhzad OC. Nanoparticles in medicine: therapeutic applications and developments. Clin Pharmacol Ther. 2008; 83:761–769. [PubMed: 17957183]
5. Allen TM, Cullis PR. Liposomal drug delivery systems: from concept to clinical applications. Adv Drug Deliv Rev. 2013; 65:36–48. [PubMed: 23036225]
6. Pasut G, Veronese FM. State of the art in PEGylation: the great versatility achieved after forty years of research. J Control Release. 2012; 161:461–472. [PubMed: 22094104]
7. Immordino ML, Dosio F, Cattel L. Stealth liposomes: review of the basic science, rationale, and clinical applications, existing and potential. Int J Nanomed. 2006; 1:297–315.
8. Sen K, Mandal M. Second generation liposomal cancer therapeutics: transition from laboratory to clinic. Int J Pharm. 2013; 448:28–43. [PubMed: 23500602]
9. Ferrari M. Cancer nanotechnology: opportunities and challenges. Nat Rev Cancer. 2005; 5:161–171. [PubMed: 15738981]
10. Hamad I, Al-Hanbali O, Hunter AC, Rutt KJ, Andresen TL, Moghimi SM. Distinct polymer architecture mediates switching of complement activation pathways at the nanosphere-serum interface: implications for stealth nanoparticle engineering. ACS Nano. 2010; 4:6629–6638. [PubMed: 21028845]
11. Kim HR, Andrieux K, Delomenie C, Chacun H, Appel M, Desmaële D, et al. Analysis of plasma protein adsorption onto PEGylated nanoparticles by complementary methods: 2-DE, CE and Protein Lab-on-chip system. Electrophoresis. 2007; 28:2252–2261. [PubMed: 17557357]
12. Gaspar R. Nanoparticles pushed off target with proteins. Nat Nanotechnol. 2013; 8:79–80. [PubMed: 23380930]
13. Lundqvist M, Stigler J, Elia G, Lynch I, Cedervall T, Dawson KA. Nanoparticle size and surface properties determine the protein corona with possible implications for biological impacts. Proc Nat Acad Sci USA. 2008; 105:14265–14270. [PubMed: 18809927]
14. Mahon E, Salvati A, Baldelli Bombelli F, Lynch I, Dawson KA. Designing the nanoparticle-biomolecule interface for targeting and therapeutic delivery. J Control Release. 2012; 161:164–174. [PubMed: 22516097]

15. Monopoli MP, Aberg C, Salvati A, Dawson KA. Biomolecular coronas provide the biological identity of nanosized materials. Nat Nanotechnol. 2012; 7:779–786. [PubMed: 23212421]
16. Monopoli MP, Walczyk D, Campbell A, Elia G, Lynch I, Bombelli FB, et al. Physical-chemical aspects of protein corona: relevance to in vitro and in vivo biological impacts of nanoparticles. J Am Chem Soc. 2011; 133:2525–2534. [PubMed: 21288025]
17. Salvati A, Pitek AS, Monopoli MP, Prapainop K, Bombelli FB, Hristov DR, et al. Transferrin-functionalized nanoparticles lose their targeting capabilities when a biomolecule corona adsorbs on the surface. Nat Nanotechnol. 2013; 8:137–143. [PubMed: 23334168]
18. Murphy RM. Static and dynamic light scattering of biological macromolecules: what can we learn? Curr Opin Biotechnol. 1997; 8:25–30. [PubMed: 9013660]
19. Pencer J, White GF, Hallett FR. Osmotically induced shape changes of large unilamellar vesicles measured by dynamic light scattering. Biophys J. 2001; 81:2716–2728. [PubMed: 11606284]
20. Hupfeld S, Moen HH, Ausbacher D, Haas H, Brandl M. Liposome fractionation and size analysis by asymmetrical flow field-flow fractionation/multi-angle light scattering: influence of ionic strength and osmotic pressure of the carrier liquid. Chem Phys Lipids. 2010; 163:141–147. [PubMed: 19900428]
21. Sabın J, Prieto G, Ruso JM, Hidalgo-Álvarez R, Sarmiento F. Size and stability of liposomes: A possible role of hydration and osmotic forces. Eur Phys J E Soft Matter. 2006; 20:401–408. [PubMed: 16957831]
22. Unsworth LD, Sheardown H, Brash JL. Protein resistance of surfaces prepared by sorption of end-thiolated poly(ethylene glycol) to gold: effect of surface chain density. Langmuir. 2005; 21:1036–1041. [PubMed: 15667186]
23. Wei J, Ravn DB, Gram L, Kingshott P. Stainless steel modified with poly(ethylene glycol) can prevent protein adsorption but not bacterial adhesion. Colloids Surf B: Biointerfaces. 2003; 32:275–291.
24. Zhang F, Kang ET, Neoh KG, Wang P, Tan KL. Surface modification of stainless steel by grafting of poly(ethylene glycol) for reduction in protein adsorption. Biomaterials. 2001; 22:1541–1548. [PubMed: 11374453]
25. Tierney KJ, Block DE, Longo ML. Elasticity and phase behavior of DPPC membrane modulated by cholesterol, ergosterol, and ethanol. Biophys J. 2005; 89:2481–2493. [PubMed: 16055540]
26. Cabral H, Matsumoto Y, Mizuno K, Chen Q, Murakami M, Kimura M, et al. Accumulation of sub-100 nm polymeric micelles in poorly permeable tumours depends on size. Nat Nanotechnol. 2011; 6:815–823. [PubMed: 22020122]
27. Soo Choi H, Liu W, Misra P, Tanaka E, Zimmer JP, Itty Ipe B, et al. Renal clearance of quantum dots. Nat Biotechnol. 2007; 25:1165–1170. [PubMed: 17891134]

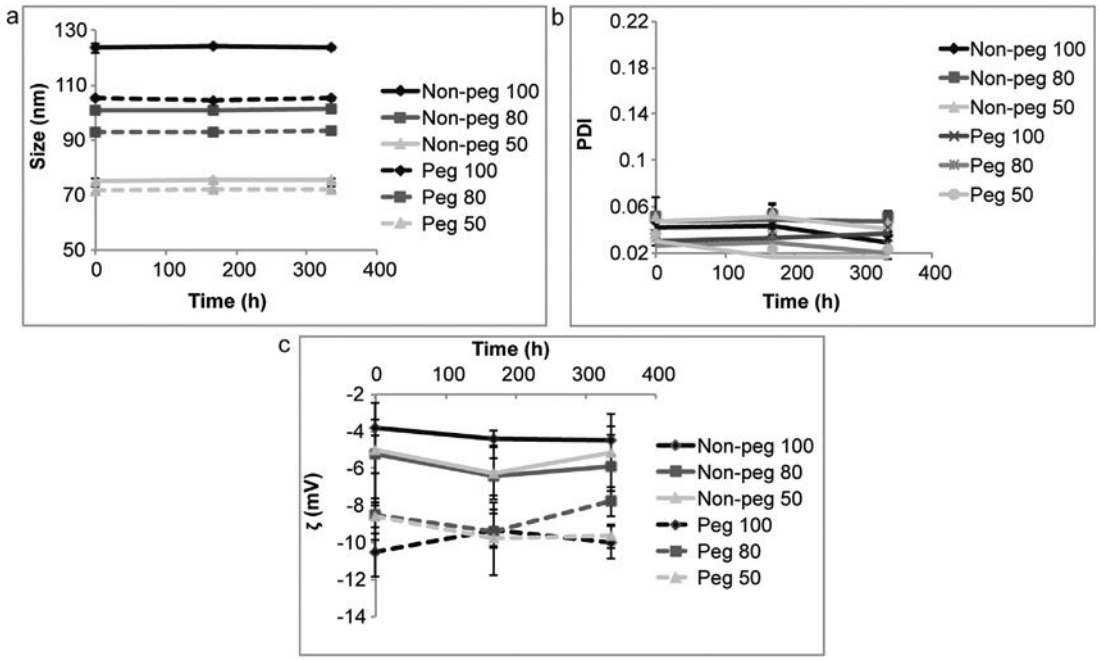

Fig. 1.

Storage stability of liposomes at 4 °C. Non-pegylated (non-peg) and pegylated (peg) liposomes were extruded through filters with 100 nm, 80 nm and 50 nm pores. (a) Size, (b) polydispersity index (PDI) and (c) zeta potential (ζ). Data is presented as mean ± SD of five measurements.

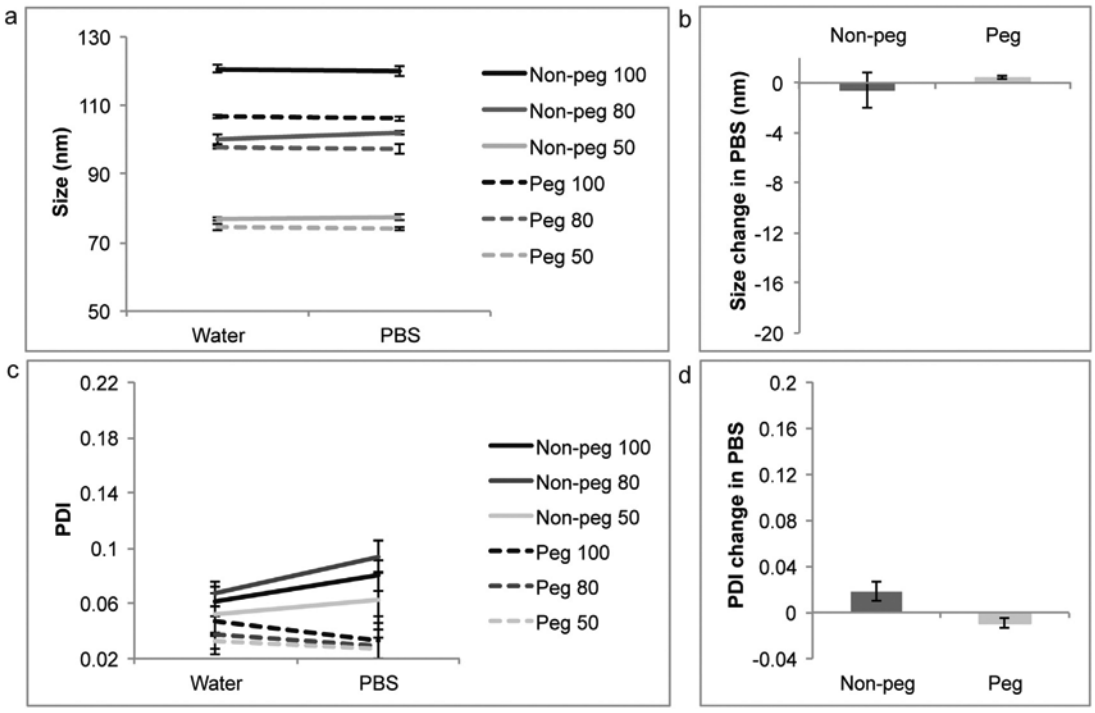

Fig. 2.

Comparison of water and phosphate buffered saline (PBS) as diluents for dynamic light scattering. Non-pegylated (non-peg) and pegylated (peg) liposomes were extruded through filters with 100 nm, 80 nm and 50 nm pores. (a,b) Size, (c,d) polydispersity index (PDI). For line graphs data is presented as mean ± SD of 5 measurements. For bar graphs data is presented as mean ± SD of liposomes with different sizes.

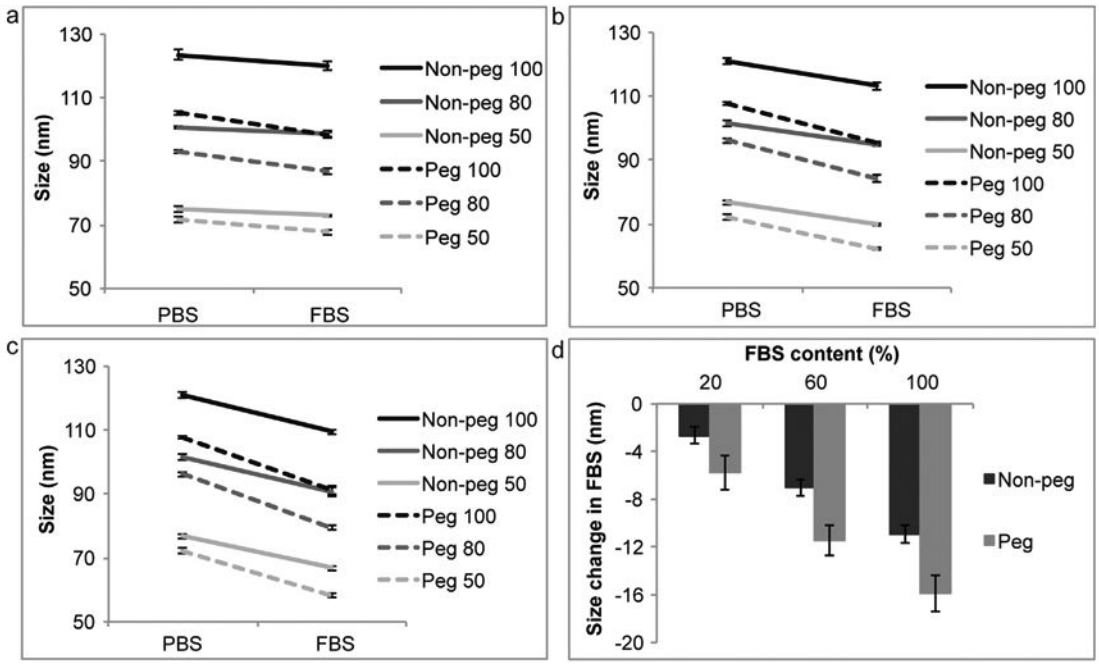

Fig. 3.

Size comparison of liposomes in phosphate buffered saline (PBS) and fetal bovine serum (FBS). Non-pegylated (non-peg) and pegylated (peg) liposomes were extruded through filters with 100 nm, 80 nm and 50 nm pores. (a) 20% FBS, (b) 60% FBS, (c) 100% FBS, (d) summarizing graph. For line graphs data is presented as mean ± SD of 5 measurements. For bar graphs data is presented as mean ± SD of liposomes with different sizes.

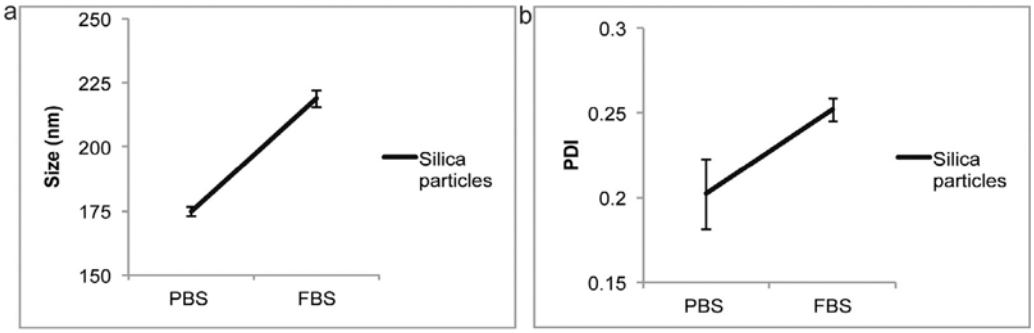

Fig. 4.

Comparison of silica nanospheres in phosphate buffered saline (PBS) and 100% fetal bovine serum (FBS). (a) Size, (b) polydispersity index (PDI). Data is presented as mean ± SD of 5 measurements.

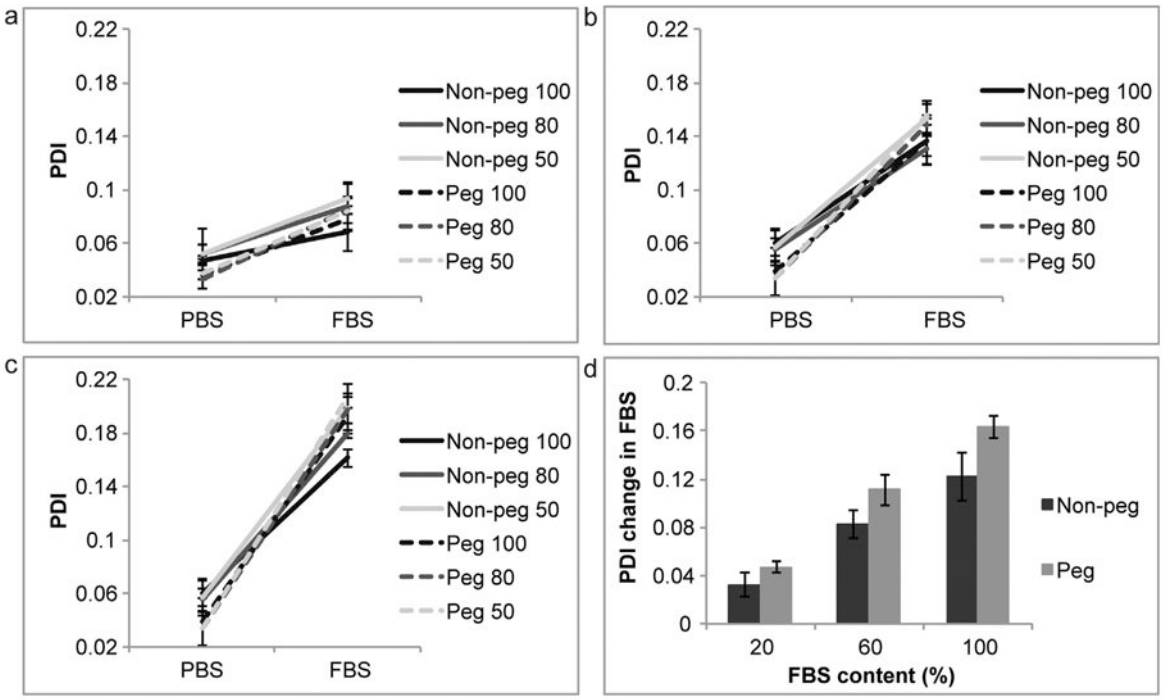

Fig. 5.

Polydispersity index (PDI) comparison of liposomes in phosphate buffered saline (PBS) and fetal bovine serum (FBS). Non-pegylated (non-peg) and pegylated (peg) liposomes were extruded through filters with 100 nm, 80 nm and 50 nm pores. (a) 20% FBS, (b) 60% FBS, (c) 100% FBS, (d) summarizing graph. For line graphs data is presented as mean ± SD of 5 measurements. For bar graphs data is presented as mean ± SD of liposomes with different sizes.

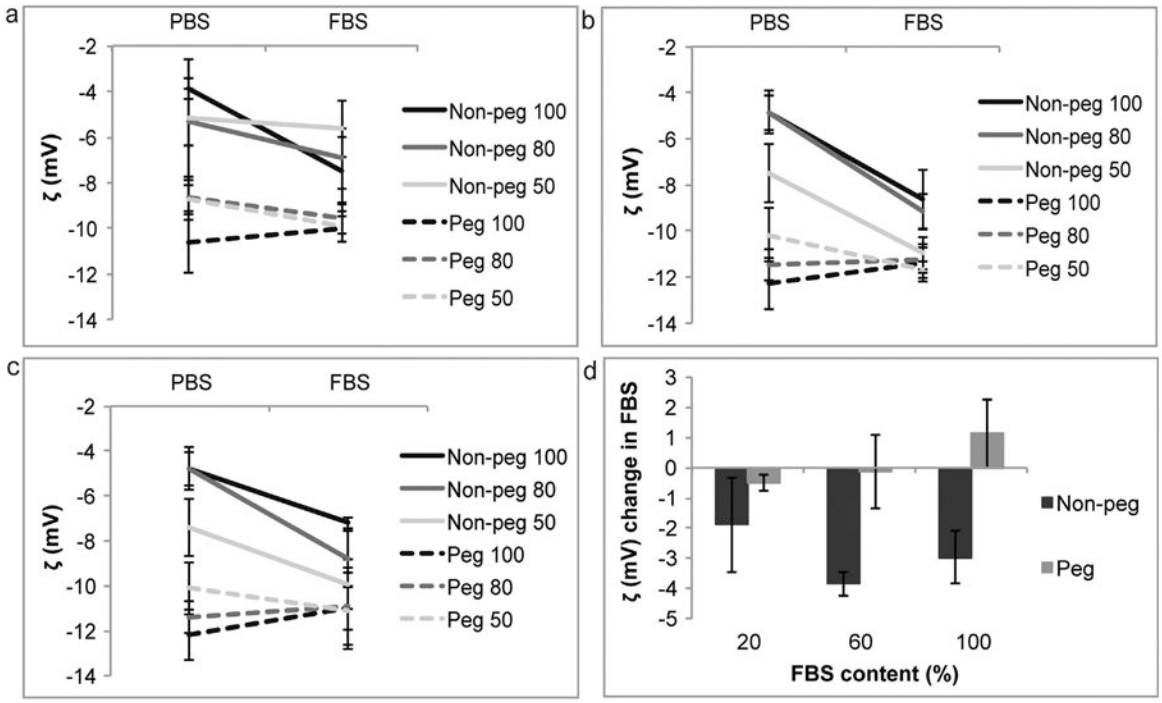

Fig. 6.

Zeta potential (ζ) comparison of liposomes in phosphate buffered saline (PBS) and fetal bovine serum (FBS). Non-pegylated (non-peg) and pegylated (peg) liposomes were extruded through filters with 100 nm, 80 nm and 50 nm pores. (a) 20% FBS, (b) 60% FBS, (c) 100% FBS, (d) summarizing graph. For line graphs data is presented as mean ± SD of 5 measurements. For bar graphs data is presented as mean ± SD of liposomes with different sizes.

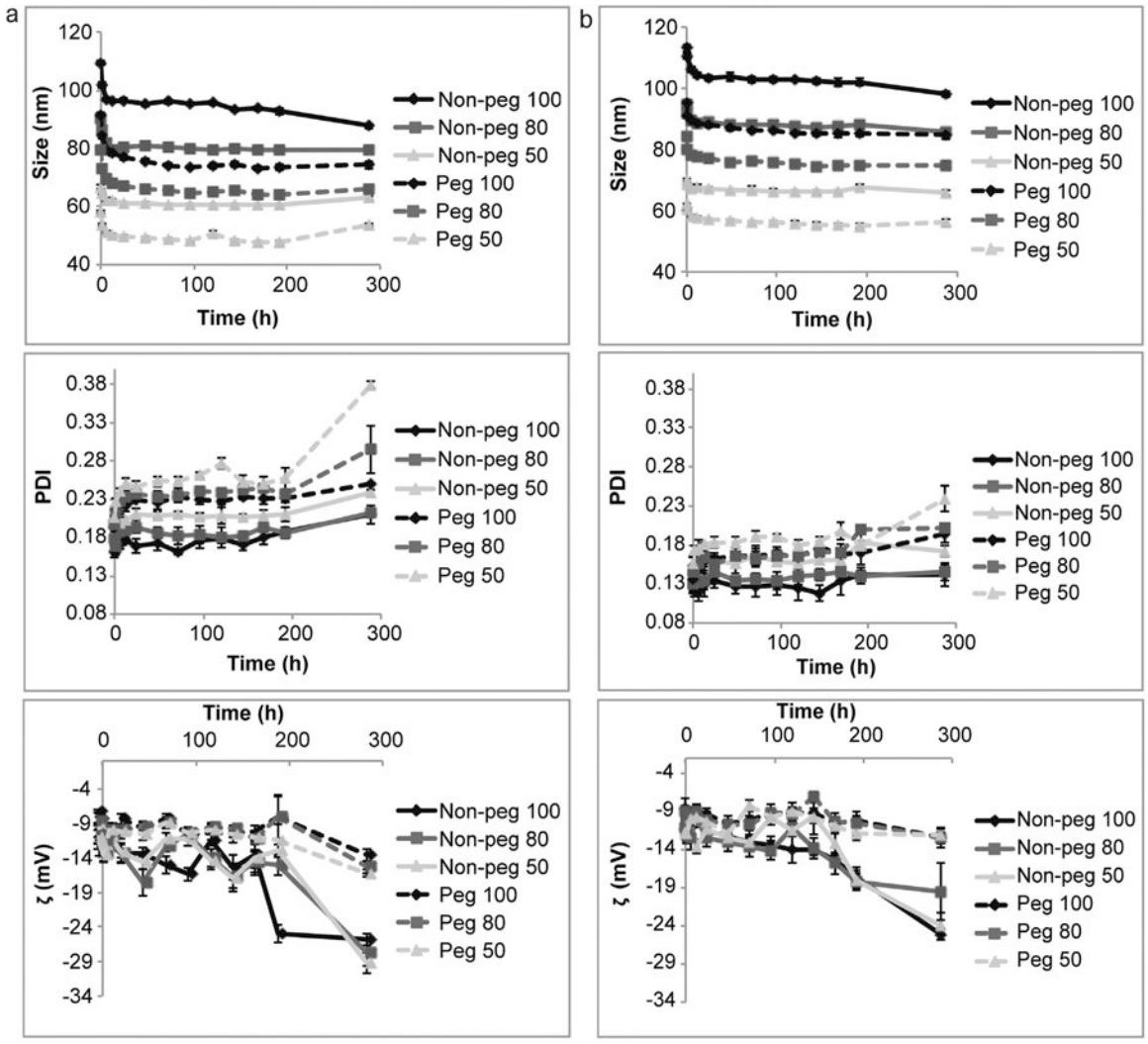

Fig. 7.

Time-course of liposomes incubated in fetal bovine serum (FBS). Non-pegylated (non-peg) and pegylated (peg) liposomes were extruded through filters with 100 nm, 80 nm and 50 nm pores. (a) 100% FBS, (b) 60% FBS. Size (upper panel), polydispersity index (PDI, middle panel) and zeta potential (ζ, lower panel) were measured. Data is presented as mean ± SD of 5 measurements. Invisible error bars are located within the symbols.

Table 1

Characterization of non-pegylated (non-peg) and pegylated (peg) liposomes. Extrusion through filters with 100 nm, 80 nm and 50 nm pores. Data is presented as mean ± SD of liposomes prepared on three separate days.

Sample	Size (nm)	Polydispersity index	Zeta potential (mV)
Non-peg 100	112.7 ± 1.5	0.056 ± 0.008	−4.9 ± 1.3
Non-peg 80	100.7 ± 0.7	0.058 ± 0.008	−5.1 ± 0.2
Non-peg 50	76.3 ± 1	0.054 ± 0.003	−5.8 ± 1.4
Peg 100	106.5 ± 1.3	0.041 ± 0.006	−10.9 ± 1.2
Peg 80	95.7 ± 2.4	0.035 ± 0.002	−10.8 ± 2
Peg 50	72.8 ± 1.4	0.034 ± 0.002	−9.3 ± 0.8